Casas, R., Gálvez, F. & Campos, M. (2018, mayo). Microstructural development of powder metallurgy cobalt-based superalloys processed by field assisted sintering techniques (FAST). Materials Science and Engineering: A, 724, 461-468.

DOI: 10.1016/j.msea.2018.04.004

Microstructural development of Powder Metallurgy Cobalt-based superalloys processed by Field Assisted Sintering Techniques (FAST)

R. Casas, F. Gálvez, M. Campos

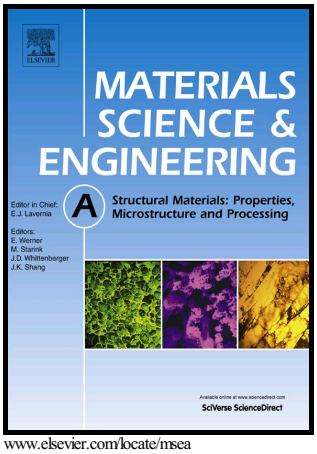

www.elsevier.com/locate/msea

PII: S0921-5093(18)30502-1
DOI: https://doi.org/10.1016/j.msea.2018.04.004
Reference: MSA36324

To appear in: *Materials Science & Engineering A*

Received date: 2 March 2018
Revised date: 16 March 2018
Accepted date: 3 April 2018

Cite this article as: R. Casas, F. Gálvez and M. Campos, Microstructural development of Powder Metallurgy Cobalt-based superalloys processed by Field Assisted Sintering Techniques (FAST), *Materials Science & Engineering A,* https://doi.org/10.1016/j.msea.2018.04.004

Microstructural development of Powder Metallurgy Cobalt-based superalloys processed by Field Assisted Sintering Techniques (FAST)

R. Casas[1 2], F. Gálvez[2], M. Campos[1]

[1] Dpt. Materials Science and Engineering, IAAB, Universidad Carlos III de Madrid (UC3M), Av. De la Universidad 30, 28911 Leganés, Spain
[2] Dpt Materials Science, Universidad Politécnica de Madrid (UPM), Calle del Profesor Aranguren s/n, 28040, Madrid, Spain

Abstract

This study reports the microstructural evolution, physical and mechanical properties of cobalt-based superalloys processed from mechanical alloyed powders and consolidated by field-assisted sintering techniques (FAST). After an initial thermodynamic simulation of the ternary diagram by Thermocalc® to determine the composition, a sequential milling process was carried out at room temperature up to 40 h milling of two different alloying systems: Co-12Al-10W (at.%) and Co-12Al-10W-2Ti-2Ta (at.%). Characterization of the powders was performed by using X-Ray diffraction, scanning electron microscope with energy-dispersive X-ray spectroscopy (EDS) and particle-size analyzer. Consolidated samples were also characterized in terms of density, microhardness and hardness. In order to promote the dual γ/γ' microstructure, both alloys were aged after solution annealing heat treatment, improving a new route of consolidation with a new level of performance.

KEYWORDS: cobalt-based superalloys; Powder metallurgy; Field-assisted sintering

1. Introduction

The need to improve efficiency in the civil aviation industry entails development of modern gas turbines with a new generation of superalloys [1][2]. The discovery of the stable ternary $Co_3(Al,W)$ intermetallic compound with an ordered $L1_2$ precipitates structures by Sato et al [3], provides a possible potential cobat-based dual phase γ/γ' microstructures for superalloy performance at high temperatures. The dual phase microstructure consists of rafted γ'-cuboidal precipitates embedded in a continuous γ-matrix. It has been widely reported that cobat-based alloys exhibit better behavior of hot corrosion, oxidation and wear resistance than Ni-base alloys [4][5][6][7][8][9]. Such alloys, however, were not used in the past because the high temperature strength is lower than Ni base alloys. Other discoveries have been reported for the cobat-based system, such as Co_3Ti with a $L1_2$ structure [10][11] and Co_3Ta (γ-structure) [12][13]. None of these systems was capable of undergoing heat treatment at high temperatures. Currently, much research has been published that focuses on the analysis of the stability of the γ'-phase [14][15][16][17], the effect of distinct alloying elements in the stabilization of the γ or γ'-phase [18][19][20][21], and the partitioning effect [22][23][24], and how alloying elements may affect properties at high temperature[19][25][26]. With addition of -Ti and -Ta

elements to the ternary system, a dual phase γ/γ' microstructure has been developed. Adding about 2 (at.%) -Ti, raises the γ'-solvus temperature by >90 ºC and phase stability and volume fraction by 20% (similar effects are observed with the addition of 2 (at.%) -Ta [22]). Both alloying elements are strong γ'-phase stabilizers [17][18], with the addition of -Ta significantly improving the high-temperature strength.

The use of CALPHAD (CALculation of PHAse Diagrams) allows new alloys to be prepared by using preliminary databases from other published researche. Although there is only a limited thermodynamic description of the phase stability of the γ' phase in the case of cobat-based superalloys, it is possible to predict the ternary compound of Co-Al-W with the data bases provided by Cui et al [27], Yang et at [28], and Zhu et at [29]. It should be noted that in the three studies the metastable γ'-phase was described as a stable one. Current research shows that it is necessary to reassess the thermodynamic description of the scheme due to the metastable condition of the γ'-phase in the Co-Al-W system [30]. Building on other works, this paper focuses on the powder metallurgy (PM) route to fabricate a novel cobat-based alloy. This is presented as a new and alternative route, giving a finer and smaller grain size with higher efficiency parameters than conventional casting routes.

2. Experimental procedure

Thermodynamic modeling (ThermoCalc 5®) was used to design the desired cobat-based superalloy by using the data base offered by Cui et al [27]. The elemental powders Co (Co6160) and W (W4105) were provided by Eurotungstene (France) and the Al powder by SultzerMetzco (AL54NS) (Switzerland). The alloying element as pure -Ta powder, 99.98 % and commercially pure -Ti powder (CPTi grade 4) with a particle size below 75 μm were provided, respectively, by Alfa Aesar Karlsruhe (Germany) and (GfE Metal und Materialien GmbH, Germany).

Once the Co alloy was defined by thermodynamic calculations, with the aim of increasing the solvus temperature of γ', the effect of -Ti and -Ta as alloying elements was examined by preparing mixtures (see: Table 1) to be mechanically alloyed afterwards. The content of -Ta and -Ti were set by following research published by Suzuki in [31]. Mechanical alloying (MA) was performed in a planetary ball mill (Planetary Pulverisette 6, FRITSCH), using hard metal Co-WC vessel and balls at a speed of 300 rpm with a ball-to-powder weight ratio of 10:1. Before the high-energy milling, the powder mixtures were mechanically blended for 30 minutes. The milling process was performed under Ar to maintain an inert atmosphere during the milling step. The vessel was continuously refilled during the process.

Table 1 Nominal composition in (at.%) of Cobalt-based superalloys examined

Label	Co	Al	W	Ta	Ti
CoAlW (Ternary)	Bal	12	10	-	-
Co-2Ti/Ta (Quinary)	Bal	12	10	2	2

Particle size distribution was characterized by a Mastersizer 2000 (Malvern, United Kingdom) to discriminate the particle size, considering the d_{50} parameter. X-Ray diffraction (XRD) was performed in a Philips Panalytical X'Pert Pro MRD system and intensity versus 2θ plots was acquired with the angular range of the region between 30° and 100°, with a step size of 0.02° and step time of 2.4 seconds per step. The crystallite size and microstrain data were obtained by the Scherrer method through using X'Pert Highscore software.

The morphology and microstructure characteristics of the milled powders were analyzed by using a SEM Philips XL-30 and FEI TENEO equipped with an EDS system. Differential thermal analysis (DTA) was performed on a Setsys Evolution TGA & DTA/DSC (Setaram), under argon atmosphere for both Co alloys from room temperature up to 1550 °C with a step rate of 5 °C min^{-1}, detecting the phase transformation and melting point.

FAHP samples were consolidated in a Gleeble 3800 equipment (Dynamic System Inc, USA), applying simultaneously pressure and temperature, a continuous alternative current of low frequency heats the material by Joule effect. Prior to consolidation, the equipment allows a dilatometry mode to optimize the final thermal cycle. The milled powder was set into a cylindrical graphite die of 10 mm diameter for the consolidation. The process was performed under vacuum ~10^{-5} Pa up to 1250 °C for 10 min with a heating and cooling rates of 100 °C min^{-1} and approx. 3 °C min^{-1} respectively. The graphite die was gripped at a load of 5 MPa inside the vacuum chamber. When the temperature achieved 800 °C, the pressure was increased up to 80 MPa (the heating and cooling rates were, respectively, 100 °C min-1 and approximately 3 °C min -1). The temperatures were recorded with a thermocouple placed, respectively, in a punch and the center of the graphite die. The densities of the consolidated samples were measured by pycnometer of He (AccuPyc II, 1340).

Once the dual phase was promoted, because the γ' and γ phase are crystalographically coherent, lattice misfit (δ) between them is an important parameter to state the hardening effect achieved depending on the morphology and composition of the precipitates. Misfit was calculated after XRD of treated samples, using the equation $\delta = 2 (a_{\gamma'} - a_{\gamma})/(a_{\gamma'} + a_{\gamma})$ [32]. Typically tends to be spherical in alloys with near-zero misfit and become with cuboidal shape as this magnitude increases. Morphology of precipitates was studied by SEM. The volume fraction of the γ/γ' phase was studied using SEM micrographs, which were analyzed utilizing ImageJ® software. All samples were chemically etched utilizing Carapella's solution to reveal the dual γ/γ' microstructure.

In order to characterize the mechanical properties of the FAHP samples at room temperatures, a Zwick Roell microhardness tester with a Vickers diamond tip and load of 200 g ($HV_{0,2}$) and 1 kg (HV 1) was used, the data was analyzed by the hardness testing software ZHu HD. Nanoidentation tests were carried out by using a MTS Nanoidenter XP with a maximum load of 360 mN. The hardness and elastic moduli were obtained by an indentation depth between 500 nm and 1250 nm. Both values were determined from the unloading part of the force-depth curves with a minimum of 30 repetitions on each sample, according to the Oliver-Pharr method[33].

3. Results and discussion

- *Thermodynamic calculations*

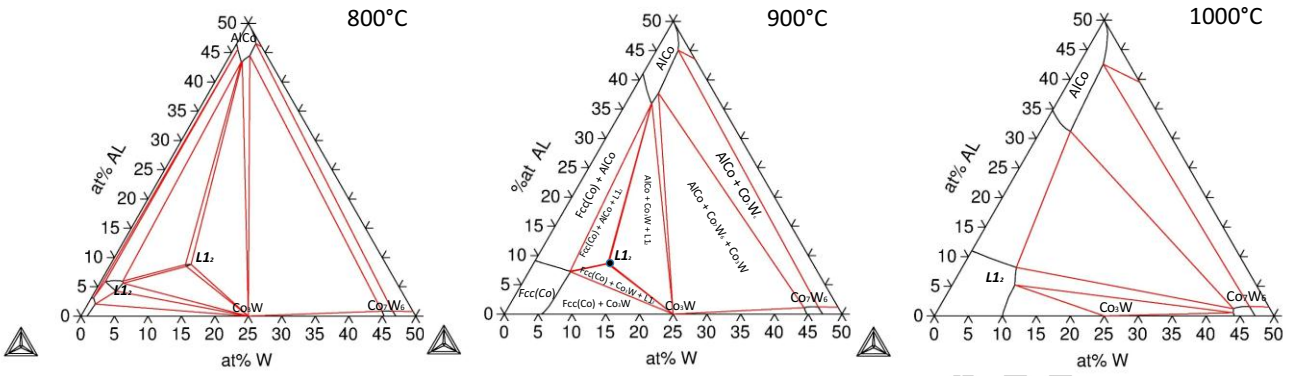

Fig. 1 Isothermal section of Co-Al-W ternary system at, , respectively, 800, 900 and 1000°C. The selected Co-Al-W composition is represented as a black point

Thermodynamic calculation provide a more precise view of the ternary phase diagram and design the optimal composition of the cobat-based γ/γ' dual phase microstructure. A ternary diagram assessment of Co-Al-W is show in Fig. 1. The phase diagram was determined by Thermocalc software® at 800, 900 and 1000 °C. It was found that γ' was stable at 800 and 900 °C. The constituent phases in the Co rich portion at 900 °C were the Co solid solution γ-(fcc Co), the β-phase (AlCo), χ-phase (Co_3W), μ-phase (Co_7W_6), and the ternary compound γ'-Co_3(Al,W) phase $L1_2$. Considering these constituents, the selected ternary composition is marked as a black point in the 900 °C isothermal section, with Co (bal), 12Al (at.%) and 10W (at.%). A higher content of aluminum was selected in order to compensate for possible losses during consolidation of future heat treatments.

- *Compositional and microstructural analysis of the powders*

The prealloyed powders were obtained by mechanical alloying (MA) methods. This process of high- energy milling simulates modifications in the Co lattice due to the operating conditions of plastic deformation, fracture, welding mechanisms, and the increase of alloying elements in the gamma Co phase. As milling time progresses, evolution of the phases became clear in the XRD patterns, showing a transformation from the common elemental peaks patterns to the gamma Co phase enriched with alloying elements and the W-phase (Fig. 2).

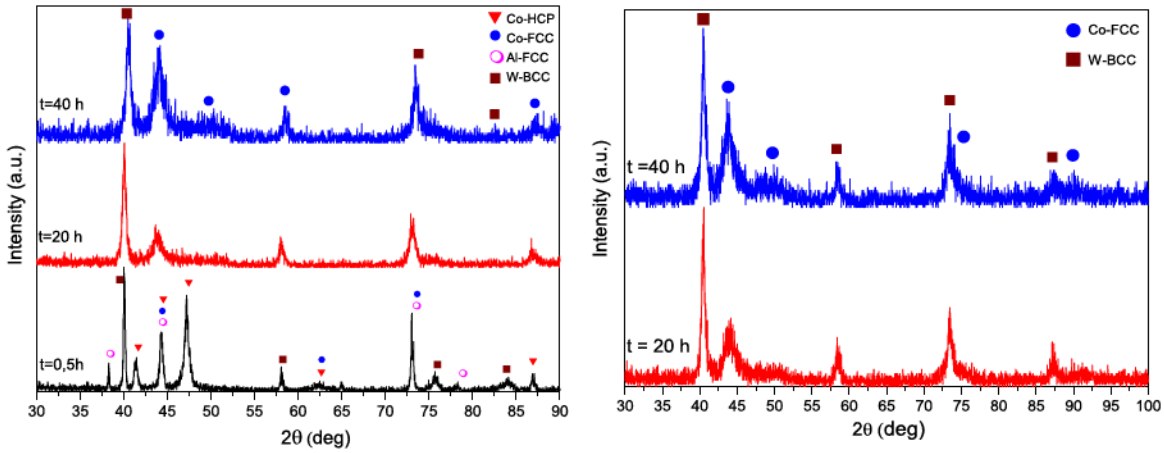

Fig. 2 XRD patterns showing the transformation from elemental powders to γ-Co fcc and W-phases with increasing milling time for ternary (left) and quinary (right) system

The crystallite size and microstrain are two crystallographic parameters sensitive to milling changes. This amount of defects generated during the milling leads to a high-dislocation density, developing subgrains recombined into the original grain. Therefore, both crystallite coherence and crystallite size decrease. The high density of dislocations, alloying processes and increase in lattice distortions produced during the milling increase the microstrain [34]. As a result of these changes, a small displacement for 2θ angle and broadening of the Bragg peaks is produced. The structural parameters of the materials obtained at different milling times is shown in Fig. 3.

A relationship between the normalized minimum grain size and the activation energy of self-diffusion has been calculated [35]. The minimum crystallite size attainable in MA is the result of a balance between the defect density induced by the high-energy milling and the recovery of the microstructure by thermal processes that took place during milling [36]. In the case of Co alloy, calculations showed a minimum grain size of 56 nm. After the MA process, ternary alloy reached approximately 75 Å and for quinary alloy <L> 54 Å. These were an indication that steady state, or a point sufficiently close to it, had been reached. For consolidation by FAHP, there was no need to increase significantly the hardness of the powder.

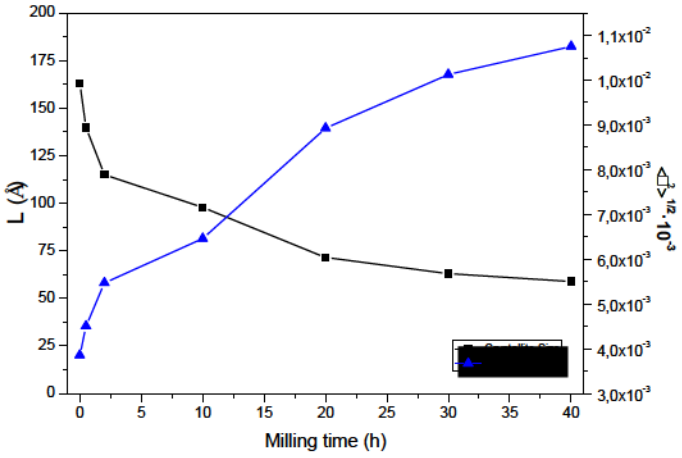

Fig. 3 Evolution of crystallite size and microstrain with milling time of Co-Al-W superalloy

Fig. 4 shows the powder particle size distribution of the ternary and quinary alloys. The average particle was centered at slightly greater sizes in the case of quinary addition. Furthermore, measurements revealed some differences regarding the d_{50} factor. For quinary, a higher parameter was also found (d_{50}=55.87 μm); and for ternary it was d_{50} = 44.80 μm. In addition, the particle sizes measured at d_{10} factor of the total powder volume were, respectively, d_{10}= 19.80 μm for ternary alloy, and d_{10}=28.16 μm for quinary alloy. The powder of both alloys was sufficiently fine, maintaining an adequate distribution to ensure good packaging and one that was necessary for the subsequent consolidation.

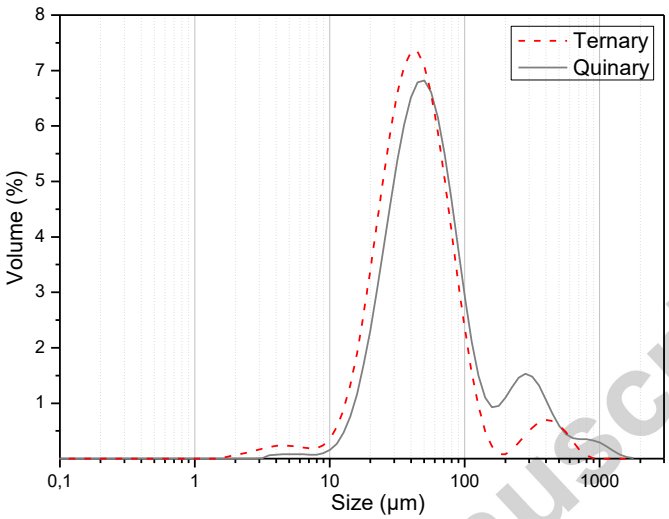

Fig. 4 Particle size distribution of ternary and quinary system powders

The SEM analysis of MA powder confirmed the phases identified by X-ray in Fig. 2. The matrix is the Co γ-phase (fcc) and the white precipitates were W-phase (bcc). Fig. 5 shows a typical evolution when a ductile material is considered together with a hard-and-brittle one [34][37]. The particles are predominantly equiaxial. Even in the case of the hardness of W elemental powder, the brighter signals underwent plastic deformation and were integrated during the ball collision with the welded particles. This observation led to an incomplete W dissolution in the Co γ-phase. The intrinsic properties of this element limited the possibility of a total alloying. It is worth mentioning that there was a small amount of MA particles in an intermediate stage (fractured) coexisting after 40 hours of milling with equiaxial MA particles that belonged to a steady state of alloying. The intermediate MA particles could decrease the densification ability during the consolidation step.

Ternary

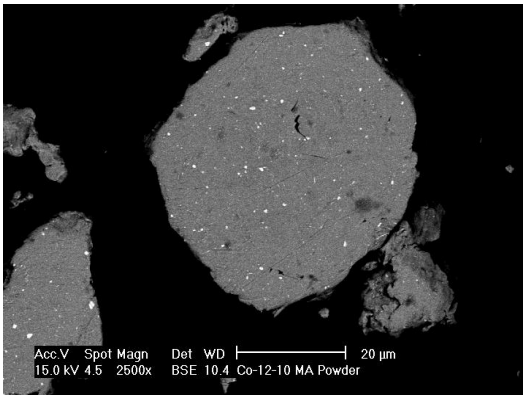

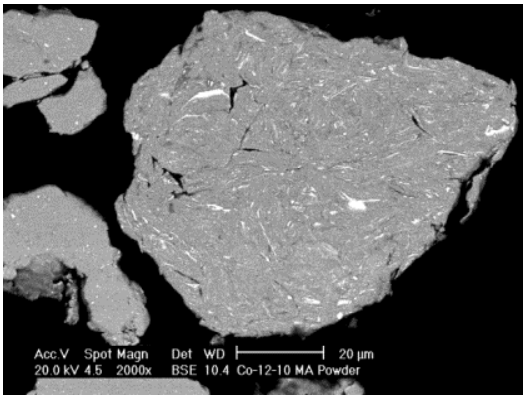

Elem	Wt %	At %
Al K	3.16	8.35
W M	31.12	12.08
Co K	65.73	79.58

Quinary

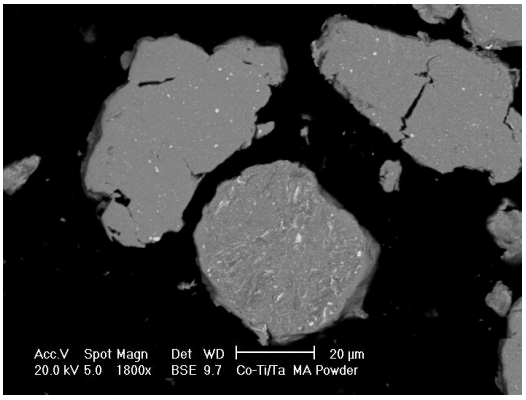

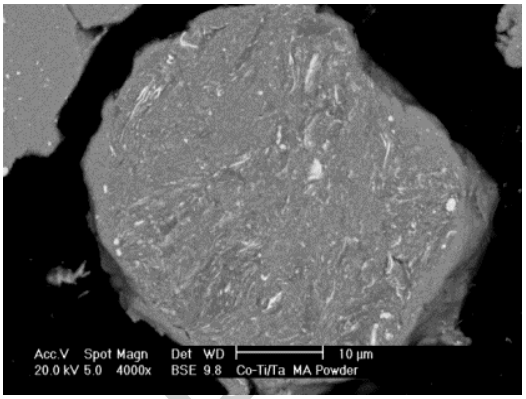

Elem	Wt %	At %
Al K	4.32	11.70
W M	35.21	14.01
Co K	59.14	73.40
Ti K	0.32	0.48
Ta L	1.01	0.41

Fig. 5 SEM micrographs of MA powders after 40 hours of milling (white areas correspond to free-W undissolved). EDS results show general particle measurements.

- *Thermal analysis of the alloyed powders*

Differential thermal analysis (DTA) was conducted for ternary and quinary powder alloys to identify heat treatments that produced the γ/γ' dual phase and transformation temperatures. The DTA of both specimens are shown in Fig. 6, where are identified the Curie temperature, the γ' solvus temperature and the melting point. Considering the Curie temperature, the thermal behavior was similar for both alloys. However, the effect of γ'-stabilizers is clearly seen when is considered the solvus T and the melting point [37]. Thanks to the presence of Ti/Ta an increase of ~ 90 °C is promoted, enhancing the stability of γ' field. In addition, $T_{melting}$ decreases with the addition of alloying elements as -Ta and -Ti. When compared with the T_{solvus} of both compositions there was an increase close to 90 °C, when -Ti and -Ta (2 %.at) elements are included in the Co-Al-W. This was a main purpose of the research given that previously works had mentioned that the addition of -Ti, -Ni and especially -Ta increase the solvus temperature.

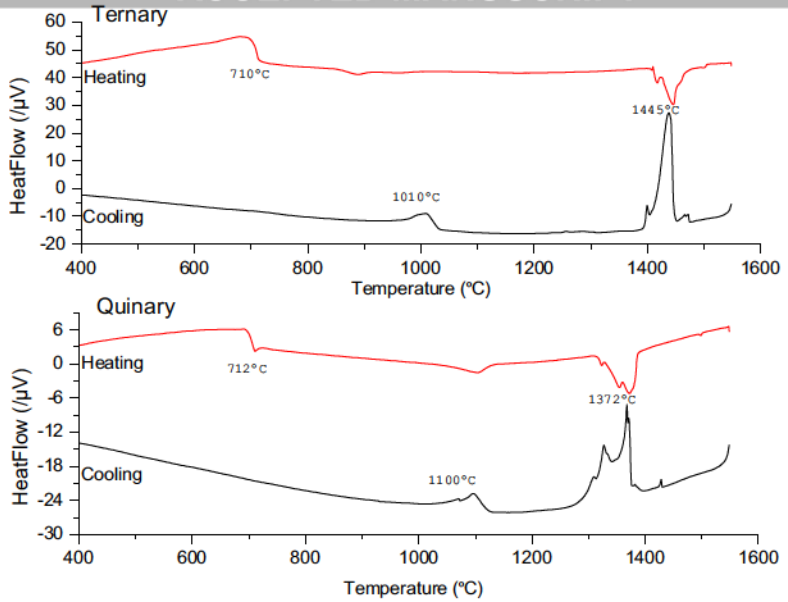

Fig. 6 Thermal analysis (DTA) for ternary (above) and quinary (below) alloys

- *Consolidation by FAHP of Cobalt-based superalloys*

In order to identify the shrinkage evolution with the T, ternary an quinary milled powder were study under the dilatometric mode recording the dimensional change at low pressure with T, Fig. 7a. As can be seen from the ternary results, there were two major shrinkages: i' on the T_{range} = 543-1173 °C with $dL/\Delta L = 2 \cdot 10^{-4}$ (%) and ii' on the T_{range} = 1173-1302 °C with $dL/\Delta L = 1{,}3 \cdot 10^{-4}$ (%). For the quinary system, there were three major shrinkages: i on the T_{range} = 616-785 °C with $dL/\Delta L = 2{,}3 \cdot 10^{-3}$ (%), ii on the T_{range} = 785-1082 °C with $dL/\Delta L = 3{,}8 \cdot 10^{-4}$ (%) and iii on the T_{range} = 1082-1288 °C with $dL/\Delta L = 7{,}9 \cdot 10^{-3}$ (%).

It is clear that the quinary system has better shrinkage as T increases, when -Ti and -Ta elements are added to the alloying system there is a sintering activation. Considering this, the FAHP cycle was designed, applying the maximum pressure once the sample has reached 800 °C and heating up to 1250 °C for 10 minutes, (see: Fig. 7b). In both cases, sintered samples reached 99% of relative density with values of 9.47 g/cm^3 for ternary system and 9.94 g/cm^3 for the quinary (measured by He pycnometer).

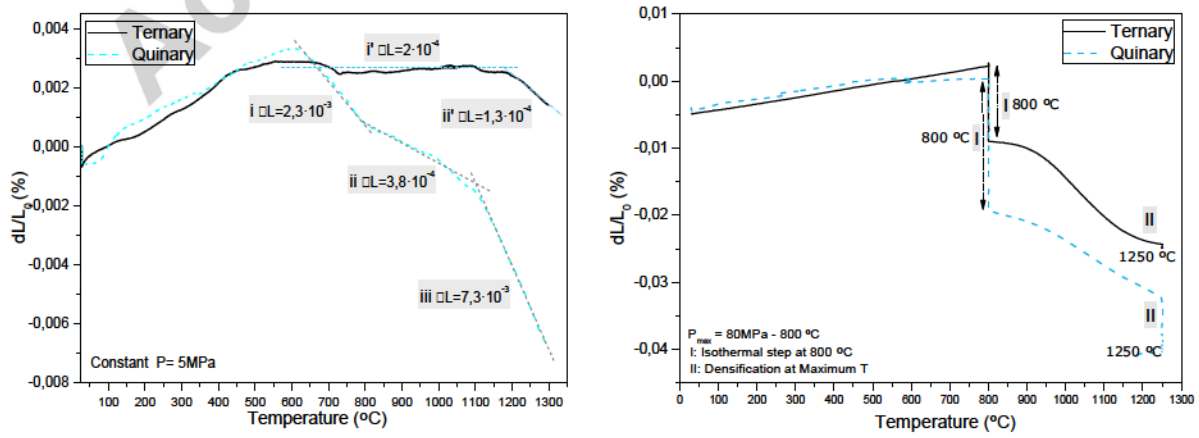

Fig. 7 a) Calculated dilatometry for ternary and quinary system vs. temperature. b) Calculated densification subjected to consolidation by FAHP

Once consolidation by FAHP had been completed, the microstructural characterization of both as-consolidated specimens was studied by X-Ray diffraction and SEM. Both compositions revealed a good densification (Fig. 8), with a γ-Co as matrix and different secondary precipitates. The white and grey precipitates in the ternary alloy is identified by EDS and XRD as η-phase (Co_6W_6C), χ-phase DO_{19}(Co_3W). In the quinary alloy, besides the η and χ phases, another secondary phase was detected, μ-phase (Co_7W_6) (see: Fig. 9). EDS measurements on this alloys have shown how –Ti and –Ta elements exhibited a partitioning behavior since –Ti was associated with Al-rich precipitates and –Ta with W-rich precipitates.

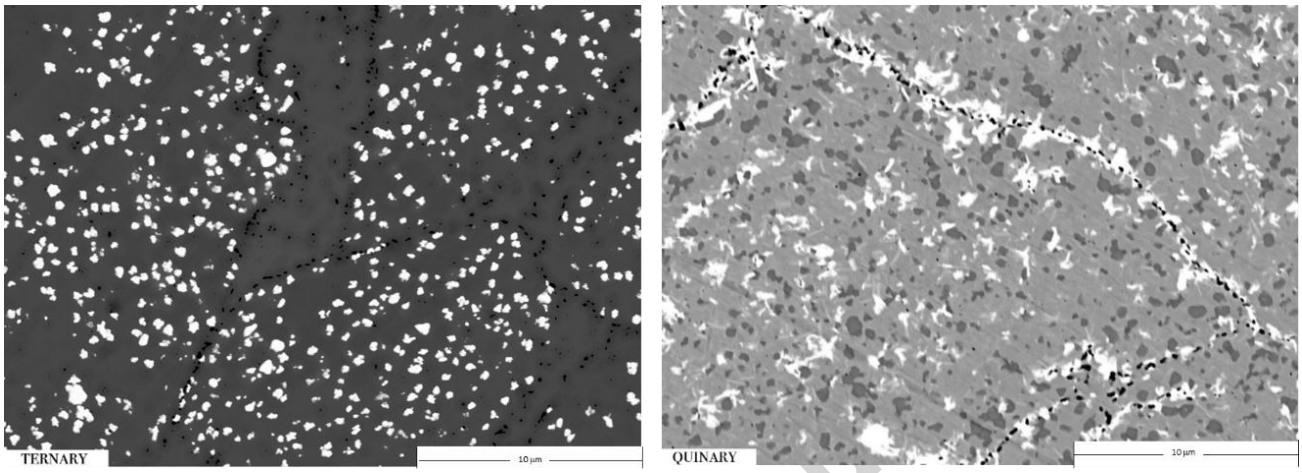

Fig. 8 Backscatter scanning electron microscopy micrographs of as-consolidated microstructure for ternary (left) and quinary (right) system

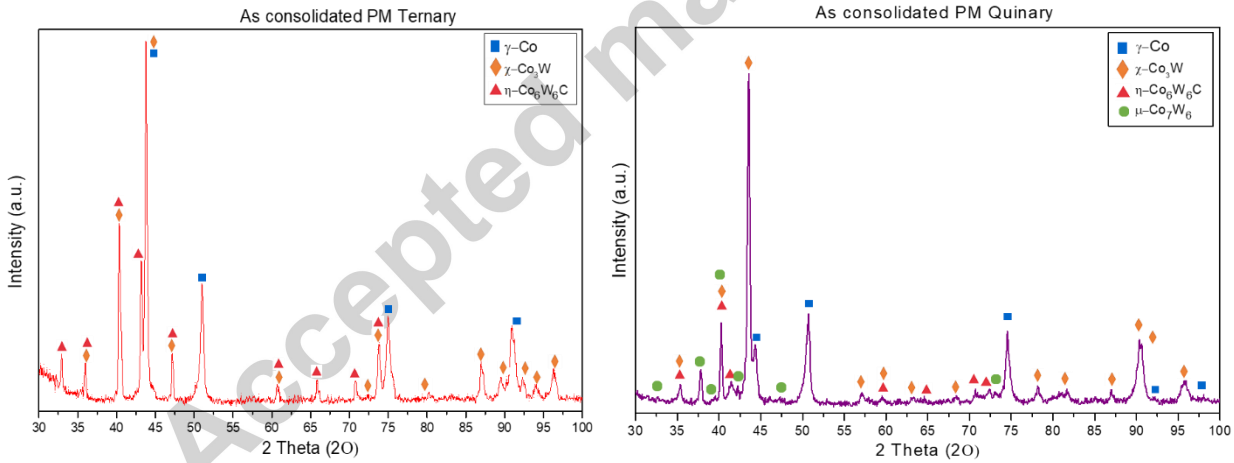

Fig. 9 Indexed X-ray diffraction patterns of as-consolidated microstructure for ternary (left) and quinary alloys (right)

In order to reach the desired γ/γ' dual phase, heat treatment was required. After the sintering, the ternary and quinary alloys underwent solution heat treatment at 1250 °C for 24 hours that entailed annealing at 900 °C for 24 hours. By using X-Ray diffractions (see: Fig. 10), it could be observed that the common peaks of the $L1_2$-phase appear at the same time as secondary phase intensities decreased for both alloys after heat treatment.

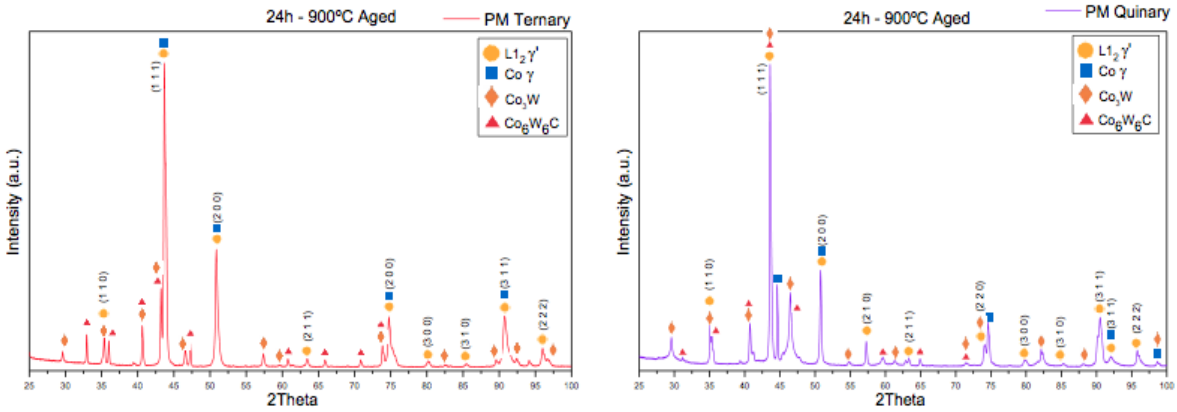

Fig. 10 indexed X-ray diffraction patterns of the ternary (left) and quinary (right) alloys after 24 hours of aging

Fig. 11 shows the microstructures by SEM micrographs with the typical cuboidal morphology of the γ'-phase in superalloys after chemical etching. The ternary compound exhibited fine cuboidal γ' precipitates of a smaller size than the quinary-cuboidal matrix. The volume fraction of the γ'-phase was 66% after solution heat treatment and 72% after 24 hours of aging heat treatment. For quinary alloy, it could be observed how the cuboidal morphology exhibited a greater degree of roughness (possibly due to the etching time). The calculated volume fraction of the γ'-phase in quinary alloy was about 56% after solution heat treatment, increasing up to 64% after aging treatment. The aging treatment increased the volume fraction of the γ'-phase in both specimens from solutionization state and was higher in the case of quinary alloys, through there were not particularly different once the thermal treatment had been performed.

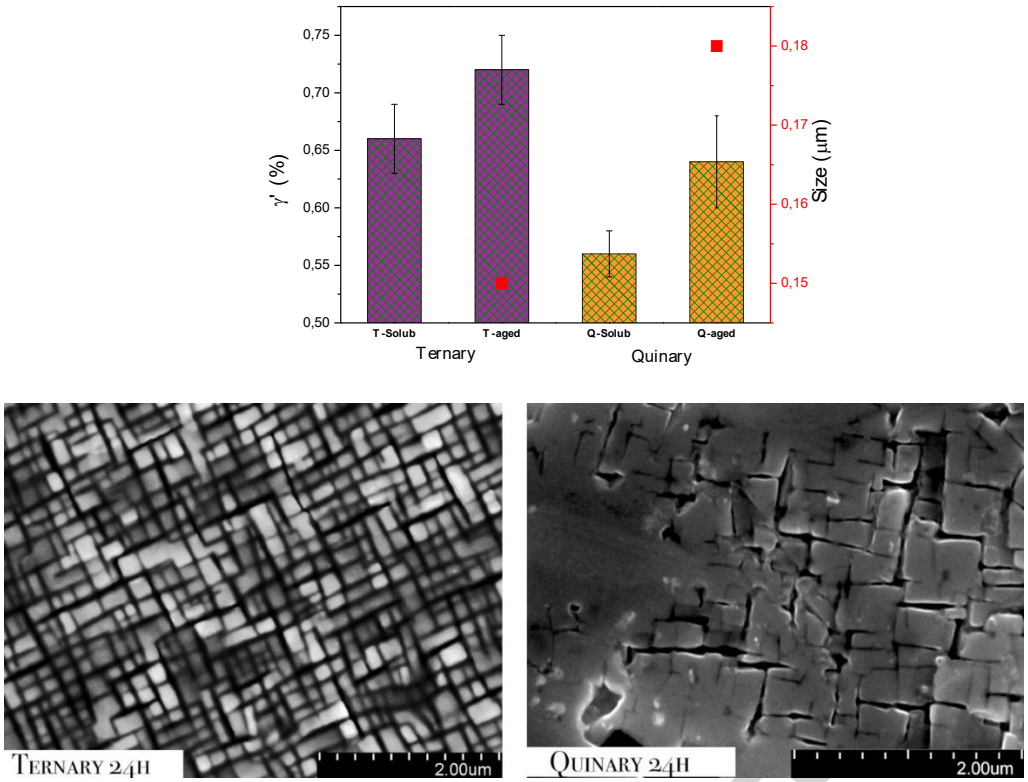

Fig. 11 Above – Volume fraction of γ'-phase (%) and cuboidal size (µm) for ternary and quinary alloys. Below – SEM micrographs of the ternary (left) and quinary (right) microstructure after 24 hours of aging

In order to examine the lattice misfit (δ) of the Co alloys, X-Ray diffractions were carried out to determine the lattice parameters of the γ-phase and γ'-phase in the ternary and quinary alloys. The (111)-reflection peak recorded at room temperature allowed calculation of the $a_{\gamma'}$ and a_{γ} parameters. These peaks exhibited an asymmetric reflection due to the existing sub-peaks coming from the γ-phase, which was lower than another sub-peak of γ'-phase. According to Sato et al, [3], cobat-based alloys possess a positive lattice misfit at room temperature. The magnitude and sign of the misfit also influence the development of microstructure under the influenced of a stress at high temperatures. The results for the ternary and quinary systems studied after heat treatments are shown in Table. 2. It can be seen that the ternary and quinary alloys increased the misfit parameters with aging heat treatments. In addition, they were higher in the case of quinary due to the alloying elements that could have changed. Similar to the findings published in [39], it could be deduced that analogous composition of ternary alloys had a similar value of misfit. In the case of addition of -Ta and -Ti elements, it could be observed that the misfit value was significantly higher than only with similar -Ti addition. It may be noted that only a small fraction of γ' was needed when the alloy was designed for service at relatively low temperatures (750 °C). [40] Other published studies have been reported that creep resistance may also be affected by γ/γ' lattice misfit, especially in Ni-base single crystal superalloys [1][4]. For Co alloys, published research has indicated that cuboidal γ' precipitates in the ternary system had comparable creep rates to Ni-base superalloy IN713C at 850 °C [22][41]

Table. 2 Recorded (111)-reflections of Co-12Al-10W and Co-12Al-10W-2Ti-2Ta after solution and aging heat treatments.

Alloy		Misfit δ
Ternary	Solution (1250-24h)	0.33
	Sol+24h aged (900-24h)	0.39
Quinary	Solution (1250-24h)	0.29
	Sol+24h aged (900-24h)	0.45

- *Mechanical behavior of FAHP cobalt-based superalloy*

The evolution of alloy hardness as a function of heat treatments is shown in Fig. 12. Microhardness results obtained at $HV_{0.2}$ showed the low porosity and favorable densification of the samples with a good mechanical response. As can be seen, additions of -Ti and -Ta elements clearly improved the hardness of the cobat-based alloys once the consolidation had been achieved. As heat treatments was carried out, the microhardness of the both alloys decreased to similar values after 24 hours of aging. This may be due to the dissolution of the secondary precipitates in to the cuboidal matrix.

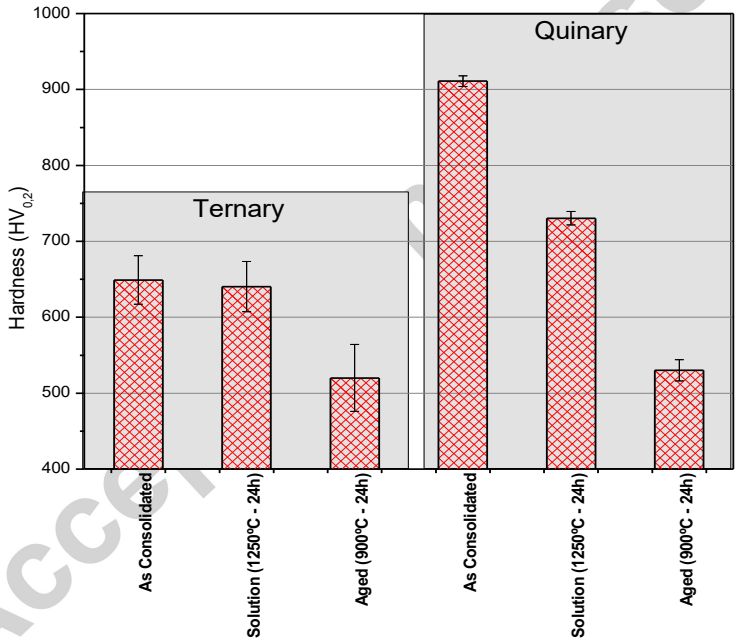

Fig. 12 Microhardness of the consolidated ternary and quinary samples

In addition, the load-displacement curves performed by nanoindentation in cobat-based samples after 24h aged were prepared, and in both systems showed an average hardness of the γ/γ' dual phase after applying a maximum load of 360 mN (see: Table. 3). Some studies have indicated that the hardness and Young's modulus of the γ'-phase increases remarkably when small additions of –Ta (~2 at.%) are added to the alloy, where the strength of the ternary system at temperature above 700 °C has been verified. [6][20][42][43]

Table. 3 Elastic modulus and hardness of the experimental Co alloys after heat treatments, determined by nanoidentation

	E_h (GPa)	H (GPa)
Ternary-A24h	(225.8 ± 20)	(6,83 ± 1.37)
Quinary-A24h	(282,2 ± 15.9)	(7.48 ± 0.63)

4. Conclusions

Cobat-based ternary and quinary superalloys can be produced following a PM route. The earlier mentioned mechanical alloying (MA) may produce powders with an almost constant composition. The consolidation was carried out by field-assisted hot pressing (FAHP), where simultaneous pressure and a continuous alternating current were applied to achieve the desired full-density specimen. Mechanical properties were analyzed. Thus, the paper offers the following conclusions:

(1) Prealloyed powder obtained by mechanical alloying depends on the particle size and relationship between crystallite size and microstrain. However, when W is included in MA-powders, it is not possible to incorporate it totally as solid solution. There is a part of W% that will remain as free element into the particles.

(2) Ternary and quinary Co alloys can be consolidated at 1250 °C by FAHP. The consolidated specimens have shown a good densification and a fine microstructure that allow a good hardness level to be achieved.

(3) In order to achieve the objective of promoting the γ/γ' dual phase, additional heat treatments have been considered (thermal solution up to 1250 °C for 24 hours and further aging at 900 °C to promote the γ' precipitation).

(4) Hardness testing showed that both alloys exhibit a good mechanical behavior compared with those examined in previous works. Undesirable secondary phases are found in the as-consolidated samples (though they are dissolved after heat treatments), showing a good cuboid shape γ' phase co-existing with the Co γ-phase matrix. It should be noted that the secondary phases are also present in small quantities after heat treatment in quinary alloys. This may be due to the difficulty associated with dissolving the alloying elements.

5. Acknowledgments

The authors acknowledge the help received from the DIMMAT project funded by the Madrid Region under the program S2013/MIT-2775.

.

References

[1] R. Reed, *The superalloys: fundamentals and applications*. Cambridge: Cambridge University Press, 2006.

[2] J. Perepezko, “The hotter the Engine, the better,” *Sci. 20*, vol. 326, no. 5956, pp. 1068–1069, 2009.

[3] J. Sato, T. Omori, K. Oikawa, I. Ohnuma, R. Kainuma, and K. Ishida, “Cobalt-Base High-Temperature Alloys,” *Sci. 312*, vol. 90, 2006.

[4] W. C. H. A.M. Beltran, in: C.T. Sims, N.S. Stoloff, “Superalloys II,” pp. 135– 163, 1987.

[5] N. T.C. Du Mond, P.A. Tully, K. Wikle, “Metals Handbook, vol. 3,” *Am. Soc. Met. Met. Park. OH*, pp. 589–594, 1980.

[6] T. M. Pollock, J. Dibbern, M. Tsunekane, J. Zhu, and A. Suzuki, “New Co-Based γ-γ′ High-temperature Alloys,” *JOM*, vol. 58, p. 62, 2010.

[7] M. S. Titus, A. Suzuki, and T. M. Pollock, “High Temperature Creep of New Ll 2 - containing Cobalt-base Superalloys,” *Superalloys 2012*, pp. 823–832, 2012.

[8] M. Tsunekane, A. Suzuki, and T. M. Pollock, “Single-crystal solidification of new Co–Al–W-base alloys,” *Intermetallics*, vol. 19, no. 5, pp. 636–643, 2011.

[9] M. Knop *et al.*, “A New Polycrystalline Co-Ni Superalloy,” *Jom*, vol. 66, no. 12, pp. 2495–2501, 2014.

[10] J. M. D. J.M. Blaise, P. Viatour, “Cobalt 49,” p. 192, 1970.

[11] D. C. P. Viatour, J.M. Drapier, “Cobalt 3,” p. 67, 1973.

[12] D. C. J.M. Drapier, J.L. de Brouwer, “Cobalt 27,” p. 59, 1965.

[13] D. C. J.M. Drapier, “Cobalt 39,” p. 63, 1968.

[14] I. Lopez-Galilea, C. Zenk, S. Neumeier, S. Huth, W. Theisen, and M. Göken, “The Thermal Stability of Intermetallic Compounds in an As-Cast SX Co-Base Superalloy,” *Adv. Eng. Mater.*, no. 6, p. n/a-n/a, 2014.

[15] Q. Yao *et al.*, “First-principles investigation of phase stability, elastic and thermodynamic properties in L12 Co3(Al,Mo,Nb) phase,” *Intermetallics*, vol. 78, pp. 1–7, 2016.

[16] P. M. Mignanelli *et al.*, “Gamma-gamma prime-gamma double prime dual-superlattice superalloys,” *Scr. Mater.*, vol. 136, pp. 136–140, 2017.

[17] K. Ishida, “Intermetallic compounds in co-based alloys-phase stability and application to superalloys,” *Mater. Res. Soc.*, vol. 1128, 2009.

[18] F. Xue, H. J. Zhou, X. F. Ding, M. L. Wang, and Q. Feng, “Improved high temperature γ’ stability of Co-Al-W-base alloys containing Ti and Ta,” *Mater. Lett.*, vol. 112, pp. 215–218, 2013.

[19] F. Pyczak *et al.*, “The effect of tungsten content on the properties of L12-hardened Co-Al-W alloys,” *J. Alloys Compd.*, vol. 632, pp. 110–115, 2015.

[20] S. Kobayashi, Y. Tsukamoto, and T. Takasugi, “The effects of alloying elements (Ta, Hf) on the thermodynamic stability of gamma prime-Co3(Al,W) phase,” *Intermetallics*, vol. 31, pp. 94–98, 2012.

[21] A. Mottura, A. Janotti, and T. M. Pollock, “Alloying effects in the gamma prime phase of Co-base superalloys,” *Superalloys 2012 12th Int. Symp. Superalloys.*, p. 685, 2012.

[22] I. Povstugar *et al.*, “Elemental partitioning and mechanical properties of Ti- and Ta-

containing Co-Al-W-base superalloys studied by atom probe tomography and nanoindentation," *Acta Mater.*, vol. 78, pp. 78–85, 2014.
[23] M. Ooshima, K. Tanaka, N. L. Okamoto, K. Kishida, and H. Inui, "Effects of quaternary alloying elements on the γ′ solvus temperature of Co-Al-W based alloys with fcc/L12 two-phase microstructures," *J. Alloys Compd.*, vol. 508, no. 1, pp. 71–78, 2010.
[24] D. J. Sauza, P. J. Bocchini, D. C. Dunand, and D. N. Seidman, "Influence of ruthenium on microstructural evolution in a model Co-Al-W superalloy," *Acta Mater.*, vol. 117, pp. 135–145, 2016.
[25] W. W. Xu *et al.*, "Thermodynamic, structural and elastic properties of Co3X (X=;Ti, Ta, W, V, Al) compounds from first-principles calculations," *Intermetallics*, vol. 32, pp. 303–311, 2013.
[26] L. Zhang, X. Qu, M. Qin, Rafi-Ud-Din, X. He, and Y. Liu, "Microstructure and mechanical properties of γ' strengthened Co-Ni-Al-W-base ODS alloys," *Mater. Chem. Phys.*, vol. 136, no. 2–3, pp. 371–378, 2012.
[27] Y. F. Cui, X. Zhang, G. L. Xu, W. J. Zhu, H. S. Liu, and Z. P. Jin, "Thermodynamic assessment of Co-Al-W system and solidification of Co-enriched ternary alloys," *J. Mater. Sci.*, vol. 46, no. 8, pp. 2611–2621, 2011.
[28] S. Y. Yang, M. Jiang, and L. Wang, "Thermodynamic Description of the γ' Phase in the Co-Al-W Based Superalloys," *Mater. Sci. Forum*, vol. 747–748, pp. 654–658, 2013.
[29] J. Zhu, M. S. Titus, and T. M. Pollock, "Experimental Investigation and Thermodynamic Modeling of the Co-Rich Region in the Co-Al-Ni-W Quaternary System," *J. Phase Equilibria Diffus.*, vol. 35, no. 5, pp. 595–611, 2014.
[30] P. Wang *et al.*, "Thermodynamic re-assessment of the Al-Co-W system," *Calphad Comput. Coupling Phase Diagrams Thermochem.*, vol. 59, no. September, pp. 112–130, 2017.
[31] A. Suzuki, G. C. DeNolf, and T. M. Pollock, "Flow stress anomalies in γ-γ' two-phase Co-Al-W-base alloys," *Scr. Mater.*, vol. 56, no. 5, pp. 385–388, 2007.
[32] T. M. Pollock and S. Tin, "Nickel-Based Superalloys for Advanced Turbine Engines: Chemistry, Microstructure and Properties," *J. Propuls. Power*, vol. 22, no. 2, pp. 361–374, 2006.
[33] W. C. Oliver, G. M. Pharr, and I. Introduction, "experiments," 1992.
[34] C. Suryanarayana, "Mechanical alloying and milling," *Prog. Mater. Sci.*, vol. 46, no. 1–2, pp. 1–184, 2001.
[35] F. A. Mohamed and Y. Xun, "On the minimum grain size produced by milling Zn-22%Al," *Mater. Sci. Eng. A*, vol. 358, no. 1–2, pp. 178–185, 2003.
[36] W. I. Eckert, J.Holzer J.C., C.E. III, and Johnson, "Structural and thermodynamic properties of nanocrystalline fcc metals prepared by mechanical attrition," *J. Mater Res*, vol. 7, p. 1751, 1992.
[37] M. Adamiak, J. B. Fogagnolo, E. M. Ruiz-Navas, L. A. Dobrzañski, and J. M. Torralba, "Mechanically milled AA6061/(Ti3Al)P MMC reinforced with intermetallics - The structure and properties," *J. Mater. Process. Technol.*, vol. 155–156, no. 1–3, pp. 2002–2006, 2004.
[38] H. Y. Yan, J. Coakley, V. A. Vorontsov, N. G. Jones, H. J. Stone, and D. Dye, "Alloying and the micromechanics of Co-Al-W-X quaternary alloys," *Mater. Sci. Eng.*

A, vol. 613, pp. 201–208, 2014.

[39] C. H. Zenk, S. Neumeier, H. J. Stone, and M. Göken, “Mechanical properties and lattice misfit of γ-γ’ strengthened Co-base superalloys in the Co-W-Al-Ti quaternary system,” *Intermetallics*, vol. 55, pp. 28–39, 2014.

[40] T. Report, “Superalloys Report,” no. January, 2016.

[41] M. S. Titus, A. Suzuki, and T. M. Pollock, “Creep and directional coarsening in single crystals of new γ-γ’ Cobalt-base alloys,” *Scr. Mater.*, vol. 66, no. 8, pp. 574–577, 2012.

[42] A. Bauer, S. Neumeier, F. Pyczak, R. F. Singer, and M. Göken, “Creep properties of different γ’-strengthened Co-base superalloys,” *Mater. Sci. Eng. A*, vol. 550, pp. 333–341, 2012.

[43] L. Shi, J. J. Yu, C. Y. Cui, and X. F. Sun, “Effect of Ta additions on microstructure and mechanical properties of a single-crystal Co-Al-W-base alloy,” *Mater. Lett.*, vol. 149, pp. 58–61, 2015.